Vietnam Journal of Science and Technology ***64***(3) (2026) 507–517
DOI: https://doi.org/10.15625/2525-2518/20734

Study on preparation of nanoemulsion based on grapeseed oil and azelaic acid by response surface methodology

Pham Thi Thu Trang[1], Trinh Hoang Nghia[2], Nguyen Thuy Chinh[3,4,*]

[1]*Faculty of Chemistry, Vietnam Military Medical University, 160 Phung Hung, Ha Dong ward, Ha Noi, Viet Nam*
[2]*Université du Québec à Trois-Rivières, 3351 Boulevard des Forges, Trois-Rivières, Québec, Canada*
[3]*Institute for Material Sciences, Vietnam Academy of Science and Technology, 18 Hoang Quoc Viet, Nghia Do ward, Ha Noi, Viet Nam*
[4]*Graduate University of Science and Technology, Vietnam Academy of Science and Technology, 18 Hoang Quoc Viet, Nghia Do ward, Ha Noi, Viet Nam*

*Email: *ntchinh@ims.vast.vn*

Received: 6 May 2024; Accepted for publication: 25 June 2024

Abstract. Azelaic acid (AzA) is widely used to treat acne, eczema, melasma, and uneven skin tone. However, the AzA has low solubility and poor skin penetration, so it often requires high doses to achieve the desired therapeutic effect. In this study, the AzA was prepared in the nanoemulsion form using grapeseed oil as an oil phase, distilled water as a water phase, and Tween 20 as a surfactant. A pseudo-ternary phase diagram was built to find the suitable range of components in the nanoemulsion. The composition of the nanoemulsion was optimized by response surface methodology (RSM) with a Box-Behnken design (BBD). The optimal conditions were found to be an oil weight percentage of 10.71 %, a water weight percentage of 56.62 %, and a Tween 20 surfactant percentage of 21.28 %. Under the optimal conditions, the mean droplet size (MDS) of the nanoemulsion reached 152.2 ± 2.7 nm, close to the predicted value of 148.908 nm. Additionally, the functional groups and ultra-violet absorption of the nanoemulsion were assessed by infrared and ultra-violet spectroscopy. The stability of the nanoemulsion versus time was also evaluated. Moreover, the inhibition activity against *Bacillus cereus* - a gram-positive bacterium - of the nanoemulsion was tested and discussed.

Keywords: grapeseed oil nanoemulsions, azelaic acid, response surface methodology, emulsion stability, *Bacillus cereus* bacterium.

Classification numbers: 2.3.1, 2.4.3.

1. INTRODUCTION

Azelaic acid (AzA) is commonly prescribed for localized skin pigmentation treatment. As a dicarboxylic acid, it has antibacterial, anti-inflammatory, keratolytic, and depigmenting properties [1]. It competitively inhibits tyrosinase and is extensively studied as a depigmenting agent. It directly inhibits melanin synthesis without affecting normal melanocytes. It possesses

antioxidant activity that supports the reduction of melanin. However, due to its low solubility and poor skin permeability, the AzA often requires a higher dosage (15-20 %) to achieve the desired treatment effectiveness [2–4]. Commercial products containing 20 % AzA in cream and gel form have led to significant unavoidable side effects such as skin irritation, redness, dryness, peeling, and erythema [5]. AzA has been widely reported to be combined with various nanocarriers. The liposomal gel containing AzA has been formulated to enhance penetration through the stratum corneum for treating acne and inflammatory acne [6]. Other formulations of AzA, including liposomal gel [6], transethosomal gel [7], ethosomes [8], liposomes [8], microemulsions [9, 10], and solid lipid nanoparticles [11–14], have been evaluated to achieve the desired transdermal properties and assess their antibacterial characteristics for effective acne treatment. The solid lipid nanoparticles carrying AzA have a size of below 200 nm and do not cause redness like commercial cream samples [14].

Recently, emulsions - systems containing liquid phases dispersed in other liquid phases - have been considered as potential nanocarriers thanks to their unique properties such as small size (from a few nanometers to tens of micrometers), high surface area, and great drug delivery/loading capabilities [15, 16]. The application of microemulsions in localized drug delivery has been studied, especially in targeting the epidermal layer [16]. Emulsion systems usually consisted of water, oil, and a surfactant, and they typically exhibited good stability [16–18]. The AzA was loaded at a rate of 5 % in different microemulsion formulations with the same oil phase, isopropyl myristate, and different surfactants/co-surfactants. The mean droplet size of these formulations ranged from 220.7 to 8674.6 nm, depending on the surfactant/co-surfactant ratio [9]. In another report, the mean droplet size of AzA-loaded microemulsions ranged between 5-150 nm, in which the oil phase consisted of oleic acid and Transcutol-P [10].

From the above literature, it can be observed that reports on AzA-loaded nanoemulsions have been limited in research, especially grapeseed oil nanoemulsions for loading AzA. The grapeseed oil – a type of natural oil – has long been utilized in the development of nanoemulsions due to their safety and ready availability [19, 20]. It is known for its high content of polyunsaturated fatty acids, specifically linoleic acid (69.6 %) and oleic acid (15.8 %), as well as vitamin E and phenolic compounds [21]. The presence of linoleic and oleic acids in grapeseed oil allows them to effectively enhance skin permeability for a wide range of active pharmaceutical ingredients, whether they are lipophilic or hydrophilic [19]. Therefore, this study aims to prepare AzA-loaded nanoemulsions from grapeseed oil. The component ratios of nanoemulsions will be optimized by response surface methodology (RSM) with a Box-Behnken design (BBD). Under optimal conditions, the stability of the AzA-loaded nanoemulsion will be assessed. Moreover, the antibacterial activity of the AzA-loaded nanoemulsion against *Bacillus cereus* bacterium - a gram-positive strain that can cause infections in the human body [22] or may be found on the skin and/or involved in skin infections [23] will also be tested and discussed.

2. MATERIALS AND METHODS

2.1. Materials

Azelaic acid (AzA, $C_9H_{16}O_4$, 98 %, flake) was provided by Bide Pharmatech, Shanghai (China). Tween 20 (density of 1.08-1.13 g/mL, saponification value of 45~55 mgKOH/g, acid value ≤ 2.0 mgKOH/g) and Tween 80 (density of 1.06-1.10 g/mL, saponification value of 45~60 mgKOH/g, pH value of 5~8) were purchased from Guangdong Guanghua Sci-Tech Co.,

Ltd. (China). Polyethylene glycol (PEG 400, average M_n 400, pH 4.5-7.5) was provided by Sigma Aldrich (USA). Pure grapeseed oil (GSO) was a commercial product of NOW Foods (USA).

2.2. Preparation of AzA-loaded nanoemulsions (AzA-NE)

AzA-NE formulations were prepared as follows: AzA was first exactly weighed and dispersed in surfactants using ultrasonication combining magnetic stirring. After the AzA was completely dissolved in surfactants, grapeseed oil was added to the above mixture, and the mixture was then vortexed for 10 minutes and ultrasonicated for 30 minutes at room temperature. Next, the distilled water was dropped slowly into this mixture before being vortexed for 10 minutes, ultrasonicated for 30 minutes and magnetic stirred for 30 minutes. This process was repeated three times to obtain a homogenous nanoemulsion system. The nanoemulsions were kept in the fridge overnight to stabilize before being determined for their properties [19, 24, 25].

2.3. Characterization

The determination of mean droplet size (MDS), polydispersity index (PI), and Zeta potential (ZP) of AzA-NE formulations was conducted using an SZ-100 nanosize analyzer (Horiba, Japan). The emulsions underwent a 100-fold dilution with distilled water [24]. The experiment was carried out in triplicate to obtain the mean value. The ultraviolet-visible transmission spectra of the AzA-NE formulation diluted 1000 times with distilled water [24] were recorded on a Libra S80 spectrometer (Biochrom, UK). The infrared spectra of the AzA-NE formulation were evaluated using a Nicolet iS10 spectrometer (Thermo Scientific, USA). The antibacterial activity of the AzA-NE formulation against *Bacillus cereus* was tested by the diffusion method on agar plates. The inhibition zone of the samples was determined after 24 hours cultured at 37 °C. A 0.25 mg/mL ampicillin solution was used as a positive control sample, while sterile RO water was used as a negative control sample.

2.4. Data analysis

The optimal process was taken on Design Expert 23.1.0 software (Stat-Ease, Inc.). The data were statistically analyzed using the analysis of variance (ANOVA).

2.5. Optimization study

The optimization was carried out by the RSM using a BBD for 15 experiments with three experiments at the center. The real variables were GSO weight percentage, Tween 20 weight percentage, and distilled water (DW) weight percentage, corresponding to A, B, and C encoding variables, respectively. The AzA dispersed in Tween 20 was fixed at 5 % as compared to the weight of the nanoemulsion. The range and center point values of three independent variables presented in Table 1 were based on the results of preliminary experiments.

Table 1. Range and center point values of three independent variables.

Real variable	Encoding variable	Variation interval (Δ)	Research level		
			-1	0	1
GSO (%)	A	10	10	20	30

Tween 20 (%)	B	20	20	40	60
DW (%)	C	20	30	50	70

3. RESULTS AND DISCUSSION

3.1. Finding suitable components for preparing AzA-NE formulations

3.1.1. Finding the suitable range of components in AzA-NE systems

The mean droplet size (MDS) and polydispersity index (PI) of AzA-loaded emulsion systems in which AzA was dispersed in different environments are presented in Table S1 (In Supporting file). The content of AzA in these systems (only 1.67 %) is quite low, so, the MDSs of these systems are small. The emulsion AzA + GSO has the highest MDS value because of the poor solubility of AzA in GSO as mentioned above. The difference in MDS of emulsion AzA + Tween from that of emulsion AzA + PEG 400 may be due to the difference in emulsifiers. PEG 400 is a co-surfactant while Tween 20 and Tween 80 are non-ionic surfactants. The non-ionic surfactants are often suitable for preparing O/W emulsions [25, 26]. The emulsion of AzA + Tween 20 exhibits the smallest MDS and standard deviation, therefore, Tween 20 was selected for further studies on the preparation of AzA-loaded emulsions. Table S2 (In Supporting file) displays the ratio of components for constructing a pseudo-ternary phase diagram that was prepared following some reports [24, 25]. From the phase diagram in Figure S2 (In Supporting file), it can be seen that, to form emulsions from GSO, DW, and Tween 20 + AzA, the range of GSO is 10-60 %, the range of emulsifier is 10-60 %, and the range of DW is 30-80 %.

To find the suitable range of components in AzA-loaded emulsions for optimization, the contents of GSO and Tween 20 were varied, while the contents of DW and AzA were fixed at 50 % and 3 %, respectively, as presented in Table 2. Based on the results of MDS, PI and ZP, it can be seen that the low content of GSO (M1) and high content of Tween 20 (M8, M9, M10) are suitable for the preparation of highly stable AzA-loaded emulsions. From there, the range of technological factors was selected as shown in Table 1.

Table 2. MDS, PI, and ZP of AzA-loaded emulsions prepared with different component ratios.

No.	GSO (%)	Tween 20/AZA (%/%)	DW (%)	MDS (nm)	PI	ZP (mV)
M1	10	20/3	50	93.6 ± 0.9	0.931 ± 0.206	-20.9 ± 3.8
M2	20	20/3	50	209.8 ± 9.1	0.160 ± 0.045	-3.2 ± 0.9
M3	30	20/3	50	327.3 ± 11.5	5.934 ± 1.961	-5.3 ± 1.0
M4	40	20/3	50	279.9 ± 6.1	0.591 ± 0.745	-5.2 ± 0.6
M5	50	20/3	50	547.2 ± 4.3	2.458 ± 1.909	-3.6 ± 4.0
M6	20	10/3	50	256.2 ± 2.7	1.230 ± 0.666	-3.8 ± 0.4
M7	20	20/3	50	209.8 ± 9.1	0.160 ± 0.045	-4.1 ± 0.7
M8	20	30/3	50	131.8 ± 1.5	0.171 ± 0.146	-54.3 ± 5.8
M9	20	40/3	50	113.6 ± 1.8	0.077 ± 0.058	-69.5 ± 2.7
M10	20	50/3	50	70.0 ± 1.3	0.254 ± 0.170	-74.3 ± 18.7

3.1.2. Optimization

Fifteen experiments were designed according to BBD, and the values of objective function - MDS - are presented in Table 3. It can be seen that the contents of the components have a

strong effect on the MDS values in these experiments, which range from 150.0 to 932.3 nm. Three experiments at the center exhibit the MDS values with a small variation, from 392.0 nm to 428.1 nm.

Table 3. Experimental levels of technological factors and MDS values of the objective function.

Std	Run	GSO (%)	Tween 20 (%)	DW (%)	MDS (nm)
10	1	0	1	-1	932.3 ± 98.0
9	2	0	-1	-1	344.5 ± 7.0
2	3	1	-1	0	207.2 ± 4.1
6	4	1	0	-1	489.1 ±15.6
14	5	0	0	0	428.1 ±5.6
1	6	-1	-1	0	161.0 ±3.0
3	7	-1	1	0	879.0 ±63.1
8	8	1	0	1	188.6 ± 3.9
4	9	1	1	0	691.9 ± 38.6
12	10	0	1	1	796.5 ± 72.6
5	11	-1	0	-1	372.3 ± 14.5
11	12	0	-1	1	150.0 ± 6.7
13	13	0	0	0	412.7 ± 14.3
7	14	-1	0	1	335.4 ± 23.7
15	15	0	0	0	392.0 ± 3.96

Based on the values of the objective function, MDS, as shown in Table 3, a quadratic process order was selected to optimize AzA-NE systems [27]. The results of the analysis of variance (ANOVA) for the quadratic model of the objective function are presented in Table 4.

Table 4. ANOVA results of the quadratic model for response.

Source	Sum of squares	df	Mean square	F-value	p-value	Remark
Model	9.31E+08	9	1.03E+08	222.42	< 0.0001	significant
A-A	3650.85	1	3650.85	7.85	0.0379	significant
B-B	7.42E+08	1	7.42E+08	1596.66	< 0.0001	significant
C-C	55727.91	1	55727.91	119.86	0.0001	significant
AB	13607.22	1	13607.22	29.27	0.0029	significant
AC	17371.24	1	17371.24	37.36	0.0017	significant
BC	861.42	1	861.42	1.85	0.2316	not significant
A^2	16981.29	1	16981.29	36.52	0.0018	significant
B^2	74093.85	1	74093.85	159.36	< 0.0001	significant
C^2	38.6	1	38.6	0.083	0.7848	not significant
Residual	2324.76	5	464.95			
Lack of fit	1668.47	3	556.16	1.69	0.3920	not significant
Pure error	656.29	2	328.14			
Cor total	9.330E+05	14				
R^2	0.9975					

Adjusted R^2	0.9930
Predicted R^2	0.9698
Adeq precision	44.6470

From the data in Table 4, it can be seen that the F-value of the model is 222.42 and the P-value of the model is less than 0.05, indicating that the model is statistically significant. The "Lack of fit" F-value of 1.69 implies that the "Lack of fit" is not significant relative to the pure error. There is a 39.20 % chance that such a large "Lack of fit" F-value could be due to noise. Non-significant lack of fit is good, suggesting that the quadratic model is suitable for fitting the data for the optimization process. The coefficient of determination, denoted as R^2, is 0.9975, indicating that this model fits the experiment. The predicted R^2 of 0.9698 is in reasonable agreement with the adjusted R^2 of 0.9930, with a difference of less than 0.2. Adeq precision measures the signal-to-noise ratio, with a ratio greater than 4 being desirable [27, 28]. In this case, the ratio of 44.6470 indicates an adequate signal. This model can be used to navigate the design space.

As observed from Table 4, the p-values of A, B, C, AB, AC, A^2, B^2, and C^2 are significant. Therefore, after the removal of insignificant terms, the quadratic equation for the optimization of emulsion is as follows:

$$\text{MDS (nm)} = 410.933 - 21.3625A + 304.625B - 83.4625C - 58.325AB - 65.9AC - 67.8167A^2 + 141.658B^2 \quad (1)$$

From Equation (1), it can be seen the linear interaction (A, B, C), double interaction (AB, BC, AC), and square interaction (A^2, B^2, C^2) effects represent different levels of influence on the objective function [27–29]. The linear interactions exhibit the strongest effect on the objective function, in which the A and C factors represent a negative effect, while the B factor represents a positive effect, corresponding to their coefficients in Equation (1). The double interactions (AB, AC) and the square interactions show a negative effect on the objective function, as indicated by their coefficients in Equation (1).

The graphs in Figure 1 show that the experimental data of the objective function are concentrated at the center line of the graphs, confirming the suitability between the experiment and the prediction.

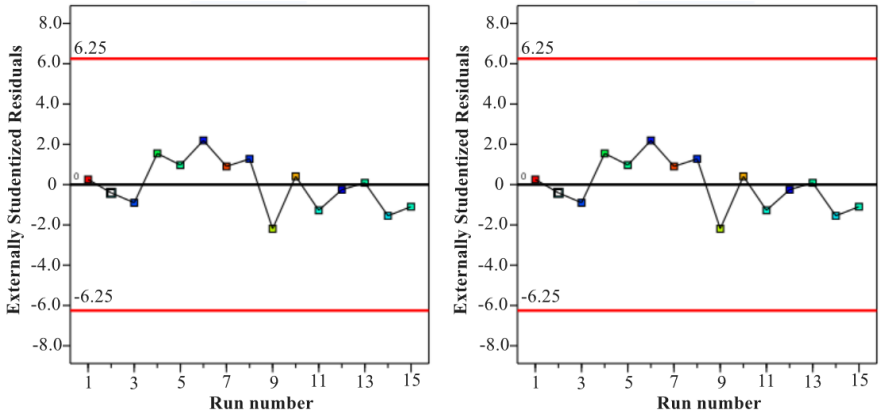

Figure 1. Graphs of predicted data vs. actual data and residuals vs. run number of 15 experiments for the optimization process.

The optimization process was set up to minimize the MDS value of the nanoemulsion and the technological factors in the range from (-1) to (+1). The level of importance for the optimization process was (+++++). The optimization solution was obtained at A = -0.929, B = -0.936, and C = 0.331 with a predicted MDS value of 148.908 nm as shown in Table 7. The response surfaces reflecting double interaction terms of encoding variables are demonstrated in Figure 2. The blue area on response surfaces is the optimal zone [29–31].

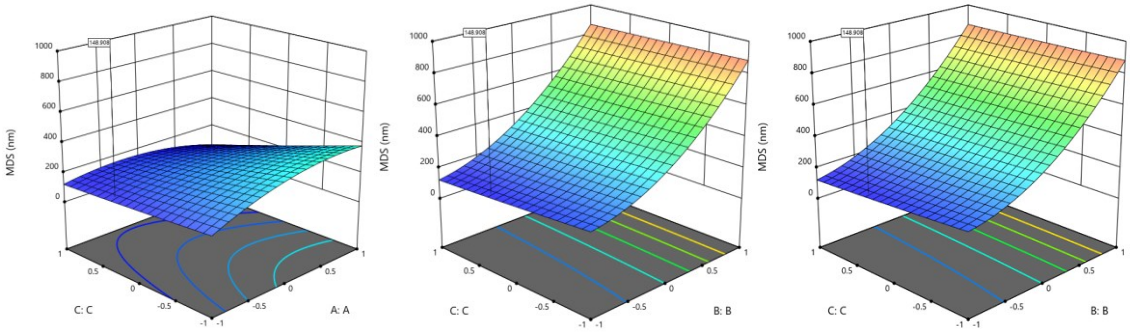

Figure 2. 3D response surfaces of double interactions on the objective function in optimization.

Table 5. Optimization results of technological variables.

Encoding variables			Real variables			Objective function (nm)	
A	B	C	GSO (%)	Tween 20 (%)	DW (%)	Experiment	Prediction
-0.929	-0.936	0.331	10.71	21.28	56.62	152.2 ± 2.7	148.908

To check the suitability between the experiment and the prediction, three experiments were repeated under optimal conditions. The MDS values of three samples prepared under optimal conditions are listed in Table 5. It can be seen that the actual MDS was close to the predicted MDS, so the experiment is suitable for the prediction.

3.2. Morphology and characteristics of AzA-NE system prepared under optimal conditions

Figure 3 presents the IR spectra of AzA, GSO, Tween 20, and AzA-NE. From the IR spectrum of AzA, the vibrations of C-H linkages were at wavenumbers of 2931, 2848, 1408, and 921 cm^{-1}, and the vibrations of -COOH were assigned at 1690 and 1249 cm^{-1} [6, 8]. The functional groups such as -OH, and -COOH were found in the IR spectra of GSO and Tween 20. From the IR spectrum of AzA-NE, the stretching and bending vibrations of hydroxyl groups were observed at 3372 cm^{-1} and 1641 cm^{-1}, respectively. Hydroxyl groups were the main groups in the AzA-NE system because of the presence of DW, AzA, GSO, or Tween 20 that contained hydroxyl groups in the emulsion. The vibrations of C-H linkages in the emulsion were assigned at 2923, 2847, 1459, 1350, and 945 cm^{-1}. The shoulder at 1742 cm^{-1} was characterized by carboxyl groups in the AzA molecule. The vibrations of C-O and C-C linkages in the emulsion were found at 1250 and 1084 cm^{-1}. The out-of-plane bending vibrations of O-H and C-H linkages in the emulsion were placed at 663 and 601 cm^{-1} [11, 19, 25].

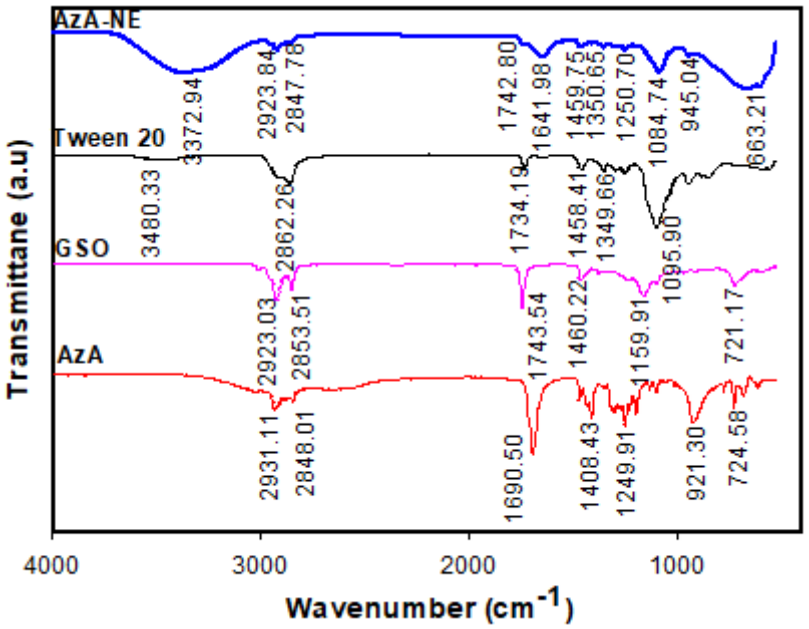

Figure 3. IR spectra of AzA, GSO, Tween 20, and AzA-NE.

Figure 4 shows the UV-Vis spectra of AzA, GSO, Tween 20, and AzA-NE, demonstrating two absorbed peaks at 204 and 230 nm, characterized by the UV absorbance of AzA, Tween 20 and GSO in the emulsion [19, 32–34].

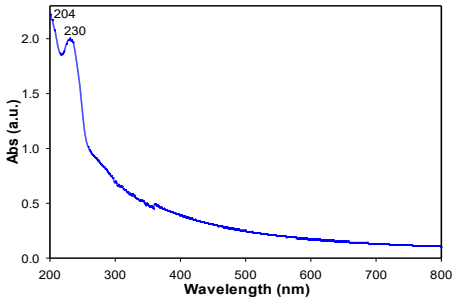

Figure 4. UV-Vis spectra of AzA-NE.

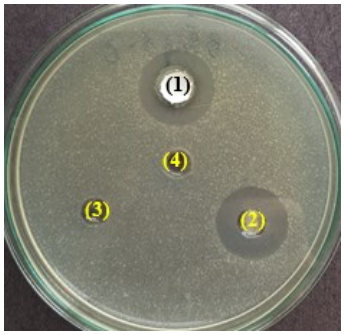

Figure 5. Antibacterial ability test image of AzA and AzA-NE after 24 hours of culture at 37 °C. (1) AzA, (2) AzA-NE, (3) ampicillin, (4) sterile RO water.

3.3. Stability of AzA-NE system

To evaluate the stability of the AzA-NE system, changes in MDS, PI, ZP, and UV transmittance at a wavelength of 800 nm (UV-T800) of the emulsion over time were recorded and the results are presented in Table 6. The changes in MDS, PI, ZP, and UV-T800 of the AzA-NE system with increasing time from 0 to 30 days were negligible, so it can be confirmed that the AzA-NE system prepared under optimal conditions exhibited high stability [24, 25].

Table 6. Changes in MDS, PI, ZP, UV-T800 over time of the AzA-NE system prepared under optimal conditions.

Time (days)	MDS (nm)	PI	ZP (mV)	UV-T800 (%)
0	152.2 ± 2.7	0.177 ± 0.083	-12.4 ± 0.2	83.29 ± 0.01
15	154.5 ± 6.8	0.213 ±0.005	-12.0 ± 0.1	81.76 ± 0.02
30	160.2 ± 4.9	0.295 ± 0.010	-11.5 ± 0.1	81.17 ± 0.15

3.4. Antibacterial activity of AzA-NE system prepared under optimal conditions

Figure 5 displays the antibacterial activity test image of AzA and AzA-NE samples after 24 hours of culture at 37 °C. It can be seen that AzA-NE and AzA can inhibit well the growth of *B. cereus* while ampicillin cannot. This bacterium is antibiotic-resistant, so it is more demanding during treatment. The diameter values of the inhibition zone of AzA and AzA-NE are 14.0 ± 0.1 and 15.0 ± 0.1 mm, respectively. This indicates that at the same AzA concentration (5 μg/μL), AzA-NE exhibits better antibacterial ability than AzA. This may be due to the nano-effect of AzA-NE, which significantly contributes to improving the antibacterial activity of the emulsion. Moreover, its great resistance against *B. cereus* together with its nanoscale size opens up the potential application of the AzA-NE system in the treatment of skin infections.

4. CONCLUSIONS

This paper presents the preparation of azelaic acid (AzA) loaded nanoemulsions from grapeseed oil (GSO) with the presence of Tween 20 as an effective surfactant. A pseudo-ternary phase diagram was set up for three components of emulsions, including GSO, distilled water (DW), and Tween 20 containing AzA. Based on the suitable range of components, the optimization process was carried out by response surface methodology and Box-Behnken design. The optimal technological variables were found with the oil phase of 10.71 %, the surfactant of 21.28 %, the water phase of 56.62 %, and the content of AzA of 5 % by weight of the emulsion. The experimental mean droplet size (MDS) of the emulsion under the optimal conditions reached 152.2 ± 2.7 nm, close to the predicted value of 148.908 nm. The AzA-loaded nanoemulsion exhibits high stability, great antibacterial ability, and small size. Therefore, the application of AzA-loaded nanoemulsions in the treatment of skin infections is promising.

CRediT authorship contribution statement. Pham Thi Thu Trang: Investigation, Methodology, Writing – original draft. Trinh Hoang Nghia: Validation. Nguyen Thuy Chinh: Supervision, Conceptualization, Writing – review & editing, Formal analysis.

Declaration of competing interest. The authors declare that they have no known competing financial interests or personal relationships that could have appeared to influence the work reported in this paper.

REFERENCES

1. Sauer N., Oślizło M., Brzostek M., Wolska J., Lubaszka K., Karłowicz-Bodalska K. – The multiple uses of azelaic acid in dermatology: mechanism of action, preparations, and potential therapeutic applications. Postepy Dermatol. Alergol., **40** (2023) 716–724. https://doi.org/10.5114/ada.2023.133955.

2. Draelos Z. D., Elewski B., Staedtler G., Havlickova B. – Azelaic acid foam 15% in the treatment of papulopustular rosacea: a randomized, double-blind, vehicle-controlled study. Cutis, **92** (2013) 306–317.
3. Thielitz A., Lux A., Wiede A., Kropf S., Papakonstantinou E., Gollnick H. – A randomized investigator-blind parallel-group study to assess efficacy and safety of azelaic acid 15% gel vs. adapalene 0.1% gel in the treatment and maintenance treatment of female adult acne. J. Eur. Acad. Dermatol. Venereol., **29** (2015) 789–796. https://doi.org/10.1111/jdv.12823.
4. Nast A., Dreno B., Bettoli V., et al. – European evidence-based (S3) guideline for the treatment of acne – update 2016 – short version. J. Eur. Acad. Dermatol. Venereol., **30** (2016) 1261–1268. https://doi.org/10.1111/jdv.13776.
5. Bergman D., Luke J. – Azelaic acid. J. Dermatol. Nurses Assoc., **9** (2017) 157–160. https://doi.org/10.1097/jdn.0000000000000309.
6. Burchacka E., Potaczek P., Paduszyński P., Karłowicz-Bodalska K., Han T., Han S. – New effective azelaic acid liposomal gel formulation of enhanced pharmaceutical bioavailability. Biomed. Pharmacother., **83** (2016) 771–775. https://doi.org/10.1016/j.biopha.2016.07.014.
7. Nasr A. M., Badawi N. M., Tartor Y. H., Sobhy N. M., Swidan S. A. – Development, optimization, and *in vitro*/*in vivo* evaluation of azelaic acid transethosomal gel for antidermatophyte activity. Antibiotics, **12** (2023) 707. https://doi.org/10.3390/antibiotics12040707.
8. Esposito E., Menegatti E., Cortesi R. – Ethosomes and liposomes as topical vehicles for azelaic acid: a preformulation study. Int. J. Cosmet. Sci., **26** (2004) 270–271. https://doi.org/10.1111/j.1467-2494.2004.00233_2.x.
9. Hung W.-H., Chen P.-K., Fang C.-W., Lin Y.-C., Wu P.-C. – Preparation and evaluation of azelaic acid topical microemulsion formulation: *in vitro* and *in vivo* study. Pharmaceutics, **13** (2021) 410. https://doi.org/10.3390/pharmaceutics13030410.
10. Salimi A., Zadeh B. S. M., Godazgari S., Rahdar A. – Development and evaluation of azelaic acid-loaded microemulsion for transfollicular drug delivery through Guinea pig skin: a mechanistic study. Adv. Pharm. Bull., **10** (2020) 239–246. https://doi.org/10.34172/apb.2020.028.
11. Shrotriya S., Ranpise N., Satpute P., Vidhate B. – Skin targeting of curcumin solid lipid nanoparticles-engrossed topical gel for the treatment of pigmentation and irritant contact dermatitis. Artif. Cells Nanomed. Biotechnol., **46** (2018) 1471–1482. https://doi.org/10.1080/21691401.2017.1373659.
12. Ghanbarzadeh S., Hariri R., Kouhsoltani M., Shokri J., Javadzadeh Y., Hamishehkar H. – Enhanced stability and dermal delivery of hydroquinone using solid lipid nanoparticles. Colloids Surf. B, **136** (2015) 1004–1010. https://doi.org/10.1016/j.colsurfb.2015.10.041.
13. Tambe V. S., Nautiyal A., Wairkar S. – Topical lipid nanocarriers for management of psoriasis–an overview. J. Drug Deliv. Sci. Technol., **64** (2021) 102671. https://doi.org/10.1016/j.jddst.2021.102671.
14. Nautiyal A., Wairkar S. – A reduced dose of azelaic acid-loaded solid lipid nanoparticles for treatment of hyperpigmentation: *In vitro* characterization and cell line studies. J. Drug Deliv. Sci. Technol., **80** (2023) 104158. https://doi.org/10.1016/j.jddst.2023.104158.
15. Zhang W., Zhang Y., He Y., Xu X., Zhao X. – Oil density and viscosity affect emulsion stability and destabilization mechanism. J. Food Eng., **366** (2024) 111864. https://doi.org/10.1016/j.jfoodeng.2023.111864.
16. Chinh N. T., Hoang T. – Review: emulsion techniques for producing polymer based drug delivery systems. Vietnam J. Sci. Technol., **61** (2023) 1–26. https://doi.org/10.15625/2525-2518/17666.
17. Giri T. K., Choudhary C., Ajazuddin, Alexander A., Badwaik H., Tripathi D. K. – Prospects of pharmaceuticals and biopharmaceuticals loaded microparticles prepared by double emulsion technique for controlled delivery. Saudi Pharm. J., **21** (2013) 125–141. https://doi.org/10.1016/j.jsps.2012.05.009.
18. Dongqi W., Daiyin Y., Junda W., Yazhou Z., Chengli Z. – Influencing factors and microscopic formation mechanism of phase transitions of microemulsion system. J. Pet. Explor. Prod. Technol., **12** (2022) 2735–2746. https://doi.org/10.1007/s13202-022-01475-4.

19. Gerber M., Oosthuysen E., van Jaarsveld J. R., Shahzad Y., du Plessis J. – Grapeseed oil nanoemulsions and nanoemulgels for transdermal delivery of a series of statins. J. Drug Deliv. Sci. Technol., **88** (2023) 104900. https://doi.org/10.1016/j.jddst.2023.104900.
20. Büyük M., Ata A., Yemenicioğlu A. – Application of pectin-grape seed polyphenol combination restores consistency and emulsion stability and enhances antioxidant capacity of reduced oil aquafaba vegan mayonnaise. Food Bioprod. Process., **144** (2024) 123–131. https://doi.org/10.1016/j.fbp.2024.01.010.
21. Jurić S., Jurić M., Siddique M. A. B., Fathi M. – Vegetable oils rich in polyunsaturated fatty acids: nanoencapsulation methods and stability enhancement. Food Rev. Int., **38** (2020) 32–69. https://doi.org/10.1080/87559129.2020.1717524.
22. Esmkhani M., Shams S. – Cutaneous infection due to *Bacillus cereus*: a case report. BMC Infect. Dis., **22** (2022) 393. https://doi.org/10.1186/s12879-022-07372-9.
23. Blaskovich M. A. T., Elliott A. G., Kavanagh A. M., Ramu S., Cooper M. A. – *In vitro* antimicrobial activity of acne drugs against skin-associated bacteria. Sci. Rep., **9** (2019) 14658. https://doi.org/10.1038/s41598-019-50746-4.
24. More S. K., Pawar A. P. – Preparation, optimization and preliminary pharmacokinetic study of curcumin encapsulated turmeric oil microemulsion in zebra fish. Eur. J. Pharm. Sci., **155** (2020) 105539. https://doi.org/10.1016/j.ejps.2020.105539.
25. Le V. T. T., Lan V. T. N., Huynh M. D., et al. – Optimizing preparation of fish scale collagen peptide/sacha inchi (*Plukenetia volubilis* L.) seed oil nanoemulsion. ChemistrySelect, **9** (2024) e202303659. https://doi.org/10.1002/slct.202303659.
26. Shen W., Koirala N., Mukherjee D., Lee K., Zhao M., Li J. – Tween 20 stabilized conventional heavy crude oil-in-water emulsions formed by mechanical homogenization. Front. Environ. Sci., **10** (2022) 873730. https://doi.org/10.3389/fenvs.2022.873730.
27. Pongsumpun P., Iwamoto S., Siripatrawan U. – Response surface methodology for optimization of cinnamon essential oil nanoemulsion with improved stability and antifungal activity. Ultrason. Sonochem., **60** (2020) 104604. https://doi.org/10.1016/j.ultsonch.2019.05.021.
28. Koocheki A., Taherian A. R., Razavi S. M. A., Bostan A. – Response surface methodology for optimization of extraction yield, viscosity, hue and emulsion stability of mucilage extracted from *Lepidium perfoliatum* seeds. Food Hydrocoll., **23** (2009) 2369–2379. https://doi.org/10.1016/j.foodhyd.2009.06.014.
29. Khatoon M., Sohail M. F., Shahnaz G., et al. – Development and evaluation of optimized thiolated chitosan proniosomal gel containing duloxetine for intranasal delivery. AAPS PharmSciTech, **20** (2019) 288. https://doi.org/10.1208/s12249-019-1484-y.
30. Kumari M., Gupta S. K. – Response surface methodological (RSM) approach for optimizing the removal of trihalomethanes (THMs) and its precursor's by surfactant modified magnetic nanoadsorbents (sMNP) - An endeavor to diminish probable cancer risk. Sci. Rep., **9** (2019) 18339. https://doi.org/10.1038/s41598-019-54902-8.
31. Huang M., Chen L., Zhang M., Zhan S. – Multi-objective function optimization of cemented neutralization slag backfill strength based on RSM-BBD. Materials, **15** (2022) 1585. https://doi.org/10.3390/ma15041585.
32. Malik D. S., Kaur G. – A validated stability-indicating RP-HPLC method for analysis of azelaic acid in pharmaceuticals. Indian J. Pharm. Sci., **80** (2018) 503–509. https://doi.org/10.4172/pharmaceutical-sciences.1000384.
33. Zhang X., Chen Y. – Photo-controlled metal-ion (Zn^{2+} and Cd^{2+}) release in aqueous Tween-20 micelle solution. Phys. Chem. Chem. Phys., **14** (2012) 2312–2316. https://doi.org/10.1039/c2cp23265k.
34. Parveen N., Sheikh A., Molugulu N., Annadurai S., Wahab S., Kesharwani P. – Drug permeation enhancement, efficacy, and safety assessment of azelaic acid loaded SNEDDS hydrogel to overcome the treatment barriers of atopic dermatitis. Environ. Res., **236** (2023) 116850. https://doi.org/10.1016/j.envres.2023.116850.